



## A FEM STUDY ON THE ADDED INERTIA OF AN OSCILLATING CYLINDER IN VISCOUS FLOW

### Daniel Rodrigo Barreto Silva

Escola Politécnica - University of Sao Paulo  
 Mechanical Engineering Department  
 Offshore Mechanics Laboratory  
 Prof. Mello Moraes Avenue, 2231 - Sao Paulo - Brazil -  
[daniel.rodriigo@usp.br](mailto:daniel.rodriigo@usp.br)

### Celso Pupo Pesce

Escola Politécnica - University of Sao Paulo  
 Mechanical Engineering Department  
 Offshore Mechanics Laboratory  
 Prof. Mello Moraes Avenue, 2231 - Sao Paulo - Brazil  
[ceppesce@usp.br](mailto:ceppesce@usp.br)

**Abstract.** *As well known, a body immersed in a fluid interacts with the surrounding flow field, through inertial and viscous forces. This work treats the classical concept of added inertia of a moving cylinder immersed in quiescent water. A brief fundamental overview is given and then the two-dimensional, laminar and unsteady flow around a circular cylinder oscillating harmonically in a resting fluid, for Keulegan-Carpenter (KC) number between 0.5 and 10, with a constant frequency parameter  $\beta$  equal to 35, is numerically addressed. The incompressible Navier-Stokes equation is solved by the finite element method, using the open source (LGPL) software FreeFem++, and the forces acting on the cylinder are calculated. The selected range of KC numbers aims to highlight the concepts of added inertia in viscous fluids, from simpler to more complex flows. The in-line force, aligned with the motion of the cylinder, is then decomposed, according to Morison equation, as a sum of inertial and drag components. The results agree well with former analytical, experimental and numerical works available in the literature. The dynamics of the flow induced by the harmonically moving cylinder is indeed rich, confirming previous results contained in the specialized literature. For low KC, the flow is symmetric and stable. For intermediate KC, the boundary layer detaches from the cylinder surface and vortices are shed at each half cycle. For higher KC, certain asymmetry develops and vortices are shed obliquely at each half cycle.*

**Keywords:** *Inertial Force, Added Mass, Forced Oscillation, Morison Equation, Freefem++*

## 1. INTRODUCTION

An immersed body in arbitrary motion interacts with the surrounding fluid. Besides viscous drag, the flow field imparts its inertial resistance to the accelerating body, as it were acted on by generalized reactive fluid forces. An increase (decrease) in the velocity of the body must be instantly accompanied by an increase (decrease) of the fluid kinetic energy, which is supplied by the body as the work of an additional resistance force, the inertial fluid force.

In analogy with Newton's second law, added mass relates the acceleration of the body with the generalized inertial fluid forces. However, in general, such generalized forces are not simply directly opposed to the body acceleration vector. In fact, unless geometric symmetries exist, acceleration in a given direction - or around a given axis - may cause reactions in - or around - other directions. The generalized inertial reactive forces are then related to the given accelerations through what is called the 'added mass tensor' or 'added mass matrix'. As a matter of fact, such a classic concept was firstly addressed in the realm of potential flows. However, this simple idealization plays a quite important role in understanding fluid-body interactions. On the other hand, the inertia force model may be used to construct indirect methods to estimate the added mass tensor, numerically or experimentally: a known acceleration is imposed to the body and the component of the generalized reactive forces in phase with the given acceleration is measured.

The concepts of added inertia occur in a variety of engineering applications in which the density of the body and medium are comparable, namely, offshore structures, ship hydrodynamics, vortex induced vibration, water impact problems, to cite some. One of the most notable added mass effects in mechanical systems is to reduce natural frequencies of vibrations.

It is not the intention of this paper to provide a full discussion on added mass concepts, but just to revisit some fundamental issues restricted to two dimensional potential and viscous flows around circular cylinders. For clearness reasons, firstly, a classical definition of the added mass tensor in potential flows, based on kinetic energy arguments, is given. Then, some considerations on the added mass concept in viscous flows are made. Finally, a numerical approach is followed. The two-dimensional incompressible Navier-Stokes equations are addressed through the finite element



method, using the open source (LGPL) software FreeFem++, for a circular cylinder which oscillates harmonically in a resting fluid for Keulegan-Carpenter ( $KC$ ) number between 0.5 and 10, with a constant frequency parameter  $\beta$  equal to 35. The in-line force is then decomposed according to the Morison equation (Morison, Johnson and Schaaf, 1950) in inertial and drag components. The selected  $KC$  numbers aims to help understanding the role of added inertia concepts in viscous fluid flows, from well-behaved to more complex ones. In the case of oscillatory motion, the added inertia has a permanent contribution to the total resistance.

## 2. ADDED INERTIA OF CIRCULAR CYLINDERS – A BRIEF OVERVIEW

### 1.1. Potential Flow and Circular Cylinder

The notion of added inertia was introduced by the studies of small oscillations of a spherical pendulum in water by Chevalier Dubuat in 1776 (Korotkin, 2010). Scientists contemporary to him worked in the experimental determination of the oscillating period of the spherical pendulum with high precision in vacuum and in a variety of mediums, like water, nitrogen, to cite some. Only Archimedes's buoyancy, the only correction applied to the problem so far, was not enough to explain the observed increase in the oscillations period. The exact expression of the added mass for a sphere was obtained by Poisson in 1831, and confirmed by George Green in 1833 (Green, 1833), for a ellipsoid, with the hypothesis of small oscillations, inviscid and incompressible fluid, in irrotational motion, namely, potential flow. Although hypothetical, the potential flow is capable to represent with certain fidelity the flow far from regions where the viscous effects are relevant. As well known, irrotational potential flows are governed by Laplace equation with appropriate boundary conditions:

$$\frac{\partial^2 \phi}{\partial x_1^2} + \frac{\partial^2 \phi}{\partial x_2^2} + \frac{\partial^2 \phi}{\partial x_3^2} = 0 \quad (1)$$

Laplace's equation is a linear elliptic partial differential equation, in which  $\phi$  is the potential function. The velocity field is easily determined as the gradient of the potential function:

$$u_i = \frac{\partial \phi}{\partial x_i} \quad (2)$$

Solutions of the Laplace's equation can be combined to form more complex flows. According to Lamb (1932), irrotational potential flows have the minimum kinetic energy and only one solution satisfying the boundary conditions is possible, contrarily to rather complex situations associated with vorticity fields (Lighthill, 1986). In principle, having the potential function of the flow around the body, it is possible to extract the added mass. Although the added inertia is strictly a dynamic phenomenon, i.e., it manifests only when the body (de)accelerates, the added mass tensor can be calculated from the potential flow around the body in uniform motion. In arbitrary motion, a rigid body has six degrees of freedom: three translational and three rotational. The induced potential function from each degree of freedom can be linearly combined:

$$\phi = \sum_{j=1}^6 U_j \phi_j \quad (3)$$

The kinetic energy of the perturbed flow due to the body movement is calculated by integrating the velocity eq. (2) over the fluid domain:

$$E = \frac{1}{2} \int_{\Omega} \rho (u_i u_i) d\Omega = \frac{1}{2} \int_{\Omega} \rho \frac{\partial \phi}{\partial x_i} \frac{\partial \phi}{\partial x_i} d\Omega \quad (4)$$

By applying the Gauss's theorem and considering eq. (1), the volume integral is transformed to a surface integral that depends on the value of the potential function and on its normal gradient at the boundaries of the domain:

$$E = -\frac{1}{2} \int_{S+\Sigma} \rho \phi \frac{\partial \phi}{\partial x_i} n_i d\Gamma = -\frac{1}{2} \int_{S+\Sigma} \rho \phi \frac{\partial \phi}{\partial n} d\Gamma \quad (5)$$



The domain is supposed to be limited externally by the contour  $\Gamma$ , far enough from the body, and internally, by the body contour  $S$ . Far from the body, the perturbation in the flow tends to nil and the gradient of the potential function vanishes at  $\Gamma$ . Consequently, eq. (5) can be written simply:

$$E = -\frac{1}{2} \int_S \rho \phi \frac{\partial \phi}{\partial n} d\Gamma \quad (6)$$

After replacing eq. (3) in eq. (6), it results:

$$E = \frac{1}{2} \sum_{i=1}^6 \sum_{j=1}^6 m_{ij} U_i U_j \quad (7)$$

With the added mass tensor defined as:

$$m_{ij} = -\rho \int_S \phi_i \frac{\partial \phi_j}{\partial n} d\Gamma \quad (8)$$

For a body immersed in a fluid extending to infinity in all directions, the added mass tensor will depend on the geometry of the body, of the fluid density and of the coordinate system only. If close to a free surface or solid (fixed or other bodies), the tensor will depend additionally on position. Usually the added mass tensor is expressed in non-dimensional form. When treating translation couplings, by dividing each term by the displaced fluid mass:

$$C_{A_{ij}} = \frac{m_{ij}}{\rho V} \quad (9)$$

or by dividing by first or by second order moments of mass when dealing with (i) translation-rotation or (ii) rotation-rotation couplings. For 2D problems, displaced fluid mass per unit length (and corresponding first or second moments) is used, instead of the displaced volume.

Consider an infinite circular cylinder translating in the directions (1, 2), perpendicular to its own axis, and rotating around it (3). The combined potential function, eq. (3), in cylindrical coordinates is given (Lamb, 1932) by:

$$\phi = U_1 \phi_1 + U_2 \phi_2 = U_i \left( \frac{D^2 \cos \theta}{4 r} \right) + U_2 \left( \frac{D^2 \sin \theta}{4 r} \right) \quad (10)$$

By replacing (10) in (8) and using the impermeability condition – the normal derivative of the potential function in (8) is made equal to the component of the cylinder velocity normal to its surface – the added mass tensor is promptly determined:

$$m_{11} = m_{22} = \rho \frac{\pi D^2}{4} \quad m_{12} = m_{66} = 0 \quad (11)$$

$$C_{A_{11}} = C_{A_{22}} = 1 \quad C_{A_{12}} = C_{A_{66}} = 0 \quad (11)$$

Geometric symmetry makes the coefficient  $m_{12}$  null, as well as  $m_{11}$  and  $m_{22}$  equal to each other. A rotation around the z axis is not capable to disturb the fluid neither to generate flow because of the tangential slip condition in potential flow at the cylinder surface summed up with the axisymmetric shape of the body. In this particular case, the added mass corresponds to the displaced fluid mass per unit length and the added mass coefficient is unitary.

## 1.2. Viscous Flow

Much has been discussed about the applicability of the previous concepts to viscous flow, in the presence or not of vortices. In potential flows, no friction (shear stress) exist between adjacent fluid layers and the fluid particles can slide relative to each other without resistance. On the other hand, frictional shear stresses occur in viscous flow. For small displacements, the potential added inertia may be a valid approximation for the initial instants of the flow, before



viscous effects take place and before boundary layer detachment (Sarpkaya, 2010). Viscosity affects significantly the topology of the flow, either through the condition at the boundaries or by the presence of free shear layers or vortices. Certainly the kinetic energy of the flow with all these features will be quite different from the potential flow.

Some non-dimensional numbers are useful to characterizing flow regimes. Given a fluid with dynamic viscosity  $\mu$  and density  $\rho$ , a body with characteristic (diameter) length  $D$  and a flow with characteristic speed  $U$ , the Reynolds number (Re), eq. (12), expresses the ratio between inertial and viscous forces. It is an indicative, e.g., of a laminar or turbulent regime, or of the development of instabilities, such as those that lead to vortex wakes.

$$\text{Re} = \frac{\rho U D}{\mu} \quad (12)$$

For an oscillating flow with period  $T$ , the Keulegan-Carpenter number ( $KC$ ), eq. (13), represents the ratio between convective and local derivatives.

$$KC = \frac{UT}{D} \quad (13)$$

The inverse of  $KC$  may be related to the well-known Strouhal number. The ratio between Re and  $KC$  results in a non-dimensional number that does not depend on the characteristic flow speed  $U$ . It is called  $\beta$  parameter, frequency parameter or even Stokes number and represents the ratio between viscous diffusion scale and flow scale, where  $\nu$  is the kinematic viscosity:

$$\beta = \frac{\text{Re}}{KC} = \frac{D^2}{\nu T} \quad (14)$$

In 1950, Morison *et al.* (1950) measured the resistance force of waves of small amplitudes on fixed circular pillars, and proposed the decomposition of the in-line force (per unit length) in two parcels, as per eq. (15). The component proportional to the acceleration corresponds to the inertial effect, while the component proportional to the velocity squared corresponds to the drag. This equation was named Morison equation and it is widely applied to express the force per unit of length on pillars and pipes. However, according to Sarpkaya (1968), Morison equation is semi-empirical and an approximate solution to a highly complex problem.

$$F_1 = -C_M \rho \frac{\pi D^2}{4} \frac{dU}{dt} - C_D \frac{1}{2} \rho D |U| U \quad (15)$$

For short periods of oscillation and small displacement amplitudes, the inertial component dominates. For long periods of oscillation and large displacements, the drag component dominates and it approximates that for the body in uniform motion. Morison equation combines these two extremes. The coefficients  $C_M$  and  $C_D$  are usually adjusted through the Fourier or the least square method, applied to the time signal of the in-line force. Inertia,  $C_M$ , and added mass,  $C_A$ , coefficients may be related as:

$$C_M = 1 + C_A \quad (16)$$

The unity originates from the pressure gradient in the mean flow that is necessary to (de)accelerate the fluid and to force it to perform an oscillatory motion.

It is also worth mentioning Stokes (1850) solution to mass and momentum conservation equations applied to incompressible fluid; respectively, Navier-Stokes and continuity equations, for a circular cylinder in oscillatory motion in a fluid at rest, for  $KC \ll 1$  and  $\beta \gg 1$ . Wang (1968) made use of asymptotic theory and expanded Stokes' solution to higher order terms. The results of Wang clearly state the dependency of the added mass and drag coefficients on viscosity through the  $\beta$  parameter:

$$C_A = 1 + 4(\pi\beta)^{-\frac{1}{2}} + (\pi\beta)^{-\frac{3}{2}} \quad (17)$$

$$C_D = \frac{3\pi^3}{2KC} \left[ (\pi\beta)^{-\frac{1}{2}} + (\pi\beta)^{-1} - \frac{1}{4}(\pi\beta)^{-\frac{3}{2}} \right] \quad (18)$$



The first two terms of the above equations correspond to Stokes' solution for a circular cylinder. In the limit  $\beta \rightarrow \infty$ , the added mass coefficient converges to its ideal (potential) value,  $C_A \rightarrow 1$ . For  $K \rightarrow 0$  and  $\beta \rightarrow \infty$ , both coefficients are related by:

$$\frac{C_A - 1}{KC \cdot C_D} = \frac{8}{3\pi^2} \quad (19)$$

By recompiling the experimental results of Keulegan and Carpenter (1958), Sarpkaya (1976) identified certain correlation between the coefficients  $C_M$  and  $C_D$  with the frequency parameter  $\beta$ . Not only the introduction of the  $\beta$  parameter ordains the experimental data notably, but it also reveals patterns, where deviation seemed to exist. Sarpkaya (1976), in a series of experiments, mapped the dependency of the drag and inertia coefficient for a wide range of  $KC$  and  $\beta$ , as resumed in figures 1 and 2, respectively. The  $\beta$  parameter figures out of fundamental importance to interpret and interpolate data. Note in figure 1 that the inertia coefficient converges to its ideal value,  $C_M = 1$ , for  $KC \lesssim 4$  and  $\beta \gg 1$ . For  $4 \lesssim KC \lesssim 12$ , a decrease (increase) of the inertia (drag) coefficient is observed, and the minimum (maximum) occurs at  $KC \approx 12$ . Sarpkaya (1977) designates this phenomenon as *inertia crisis*.

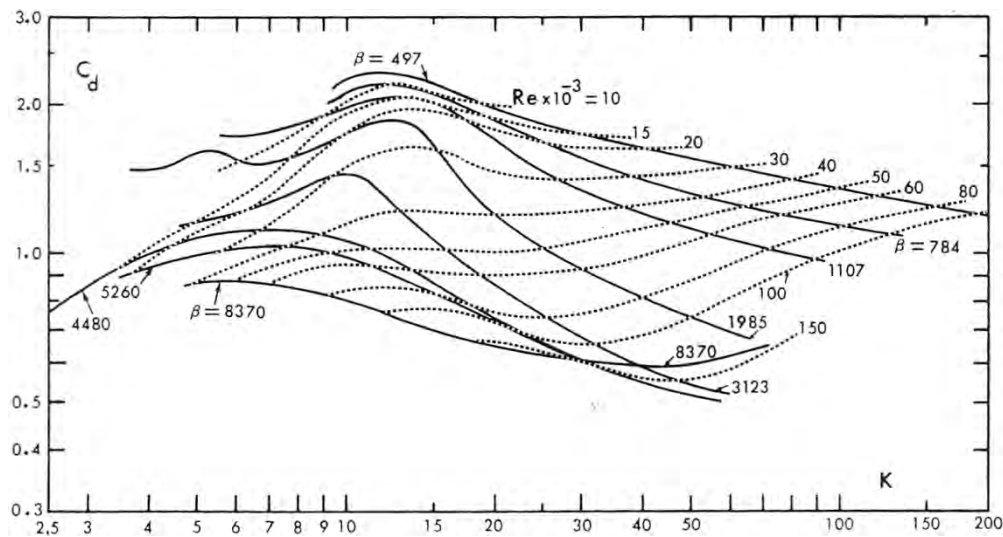


Figure 1. Drag coefficient (Sarpkaya, 1977)

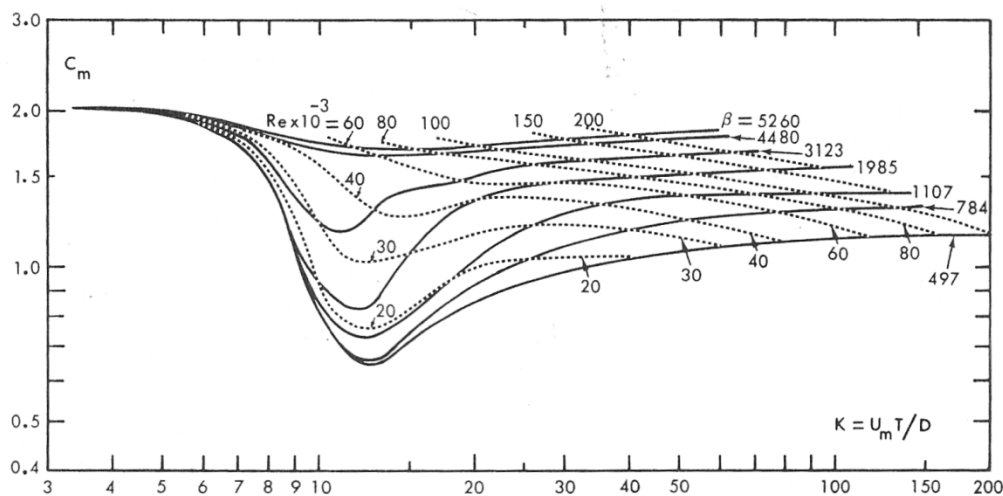


Figure 2. Inertia coefficient (Sarpkaya, 1977)

There are major differences between oscillatory and uniform flow around a circular cylinder. In an oscillating flow, the vortex shedding depends not only on  $Re$ , but also on  $KC$ . In an uniform flow, vortices are always convected downstream the cylinder, while in an oscillating flow, the vortices formed on the previous half cycle can contour the

cylinder, when the flow changes direction, and therefore interact with the vortices that are formed on the other side. This wake reversal, or wake reencounter, affects the further vortex formation and changes significantly the forces in-line and normal to the movement (Lin, Bearman and Graham, 1996).

Tatsuno and Bearman (1990) studied the topology of the flow for  $KC < 15$  and  $\beta < 150$ . They identified eight flow regimes, as depicted in figure 3. The flow regimes depend weakly on  $Re$ , and, in some range, they depend exclusively on  $KC$ . With exception to regimes A and A\*, the flows are three-dimensional.

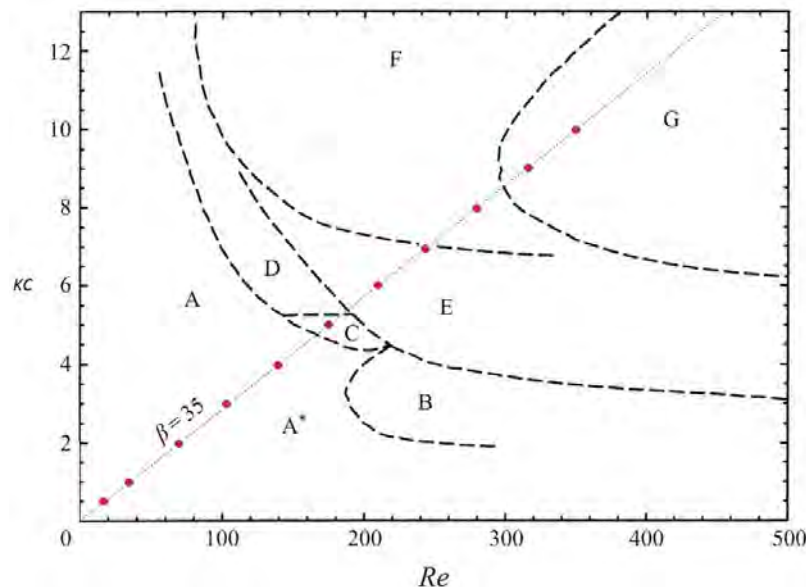


Figure 3. Flow regimes. Adapted from Dütsh et al. (1998)

- **Regime A\*:** Symmetric flow with attached boundary layer
- **Regime A:** Symmetric flow with detached boundary layer vortex formation
- **Regime B:** Honji vortices span along the cylinder length
- **Regime C:** Asymmetric flow with wake formation
- **Regime D:** Asymmetric flow with transverse vortex street
- **Regime E:** Asymmetric flow with alternating transverse vortex street
- **Regime F:** Asymmetric flow with diagonal vortex street
- **Regime G:** Asymmetric flow with diagonal vortex street

### 3. NUMERICAL SIMULATION

The cylinder is forced to oscillate harmonically in the horizontal axis with the fluid boundary sufficiently far from the cylinder at rest. The resulting flow is investigated for  $Re$  and  $KC$  in the ranges  $17.5 \leq Re \leq 350$  and  $0.5 \leq KC \leq 10$ , with a constant frequency parameter,  $\beta = 35$ . The selection of  $KC$  numbers aims to understand the concepts of added inertia in viscous fluid flow, from simpler to more complex ones. The complexity of the flow increases with  $KC$  as can be seen by tracing the line  $\beta = 35$  and the points of the numerical simulation at the map of Tatsuno and Bearman, Figure 3.

To evaluate the flow around the oscillating circular cylinder, a precise and robust numerical tool is necessary. For that, the open source (LGPL) software FreeFem++, version 3.20, was chosen. This software is developed and maintained by Prof. Frédéric Hecht of the Pierre and Marie Curie University of Paris. FreeFem++ is able to solve elliptic, parabolic and hyperbolic partial differential equations, formulated in the weak form by the Finite Element Method. The flow around blunt bodies are, in general, unsteady, with free shear layers and vortices. The interaction of the flow with the moving body demands high computational efforts.

The fluid motion is governed by the continuity and the Navier-Stokes equations, differential forms of the mass and linear momentum conservation laws, respectively. In the present work, an algorithm proposed by Li et al. (2000) for simulating the flow of a body in arbitrary motion, translation plus rotation, was used. A non-inertial coordinate system



is attached to the cylinder and the Navier-Stokes equations are written in this movable coordinate system. There are some advantages in this approach, e.g., fixed mesh and simple implementation. On the other hand, the boundary conditions of the fluid far from the cylinder must be updated at each time step. The continuity and Navier-Stokes equations are written, respectively:

$$\frac{\partial u_i}{\partial x_i} = 0 \quad (20)$$

$$\frac{\partial u_i}{\partial t} + u_j \frac{\partial u_i}{\partial x_j} = -\frac{\partial p}{\partial x_i} + \nu \frac{\partial^2 u_i}{\partial x_j \partial x_j} - \ddot{i}_i \quad (21)$$

where the last term of the Navier-Stokes equation corresponds to the inertia force introduced by acceleration of the non-inertial coordinate system. Its harmonic motion is described by:

$$r_1 = U \cdot \cos\left(\frac{2\pi}{T}t\right) \text{ and } r_2 = 0 \quad (22)$$

An integral formulation of the Navier-Stokes equation is needed for the application of the finite element method. Equation (21) is multiplied by a test function  $\delta u_i$  and it is integrated over the (limited) domain  $\Omega$ :

$$\int_{\Omega} \delta u_i \left( \frac{\partial u_i}{\partial t} + u_j \frac{\partial u_i}{\partial x_j} \right) d\Omega = \int_{\Omega} \delta u_i \left( -\frac{\partial p}{\partial x_i} + \nu \frac{\partial^2 u_i}{\partial x_j \partial x_j} - \ddot{i}_i \right) d\Omega \quad (23)$$

Gauss's theorem is then applied on the diffusive and pressure terms:

$$\int_{\Omega} \delta u_i \left( \frac{\partial u_i}{\partial t} + u_j \frac{\partial u_i}{\partial x_j} \right) + \nu \frac{\partial \delta u_i}{\partial x_j} \frac{\partial u_i}{\partial x_j} - p \frac{\partial \delta u_i}{\partial x_i} d\Omega = \int_{\Gamma} \delta u_i \left( -pn_i + \nu \frac{\partial \delta u_i}{\partial x_j} n_j \right) d\Gamma - \int_{\Omega} \delta u_i \ddot{i}_i d\Omega \quad (24)$$

A similar process is applied for the continuity equation. Equation (20) is multiplied by a test function  $\delta p$  and integrated over the domain  $\Omega$ :

$$\int_{\Omega} \delta p \frac{\partial u_i}{\partial x_i} d\Omega = 0 \quad (25)$$

The domain is partitioned (meshed) in a finite number of subdomains and nodal discrete points, in which the solution is sought, figure 4. Inside these subdomains, the solution is approximated by a linear combination of velocity and pressure values at the nodes, through interpolation functions. The interpolation functions approximate the solution inside the subdomains by linear or quadratic polynomials; they are equal to unit at the nodes, alternately, and identically null outside the subdomain.

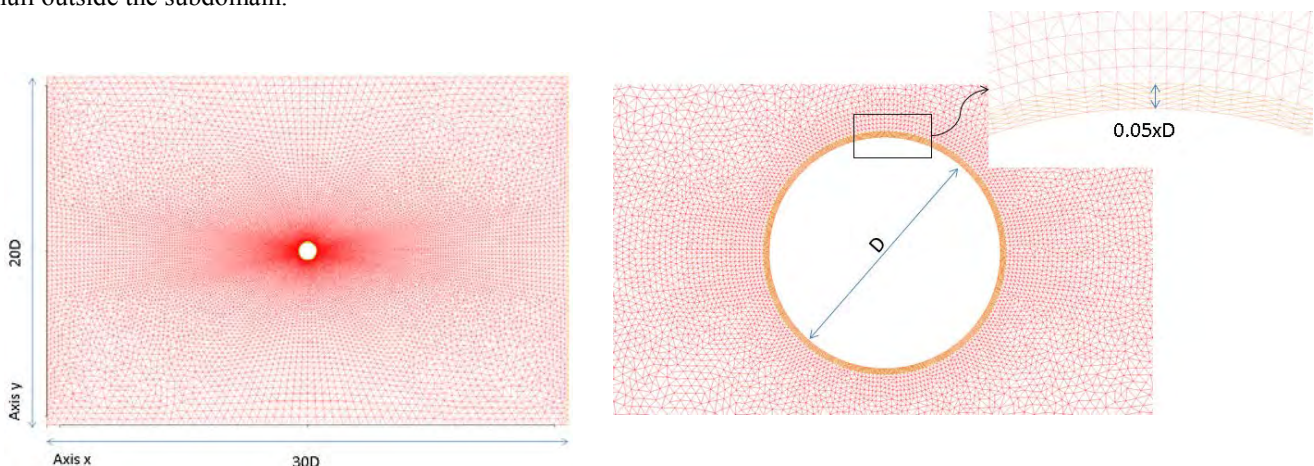


Figure 4. Mesh (left) and detail (right) around the cylinder



In the oscillating coordinate system, the boundary condition at the cylinder surface reduces to the non-slip condition. At the outer contour, far from the cylinder, the fluid is 'seen' from the cylinder reference frame as oscillatory, with velocity equal but opposite to the non-inertial coordinate system.

The great flexibility of the method lies on its diversity of available finite elements and on permitting a local refinement of the mesh in the regions with complex shapes or where high gradients in the solution are expected. The present work adopted triangular elements with 3 nodes per edge (total of 6 nodes), named  $P_2P_1$ . It is a classical element, widely tested and stable (Gresho and Sani, 2000). The velocity and the pressure fields are approximated, respectively, by quadratic and linear polynomials. Therefore, velocity and pressure are continuous functions across the elements.

Additionally, the mixed formulation, also known as u-p method, was used. The discrete equations of continuity and Navier-Stokes are solved simultaneously. The formulation of the original problem is therefore hold, resulting an algebraic system, increased in size and degree sparseness, to be solved.

Implicit methods are well-known for their stability. To advance in time, the second order backward differentiation formulae was chosen and the temporal derivative of the velocity at time step  $t_{n+1}$  estimated from the derivative of the interpolation polynomial which passes through the points  $t_{n+1}$ ,  $t_n$  and  $t_{n-1}$ , (Ferziger, 1998). It is a multi-step method that uses the information from the latest two time steps.

The combination of the backward differentiation formulae in time with finite elements  $P_2P_1$  in space results in a second order numerical method in time and space. In order to start the method, the implicit Euler method was used for the first two time steps.

#### 4. RESULTS

The in-line and normal forces were evaluated and stored for all time steps. The drag and inertia coefficients of the Morison equation were adjusted by the least squares method. The results are shown in figure 5. They agree well with the works of Stokes (1850), Wang (1968), Dütsh et al (1998) and Uzunoğlu et al (2001). The drag coefficient decays rapidly and, from  $KC=2$  on, starts deviating from the predicted values. It is important to emphasize that the asymptotic results by Stokes (1850) and Wang (1968) are based on a flow with an attached boundary layer and without vortices. Similarly, the inertia coefficient remains approximately constant and close to its asymptotic theoretical value and, for  $KC \geq 2$ , decreases and deviates from the analytical values. Boundary layer separation was initially detected for  $KC=3$  at the position of maximum speed of the cylinder.

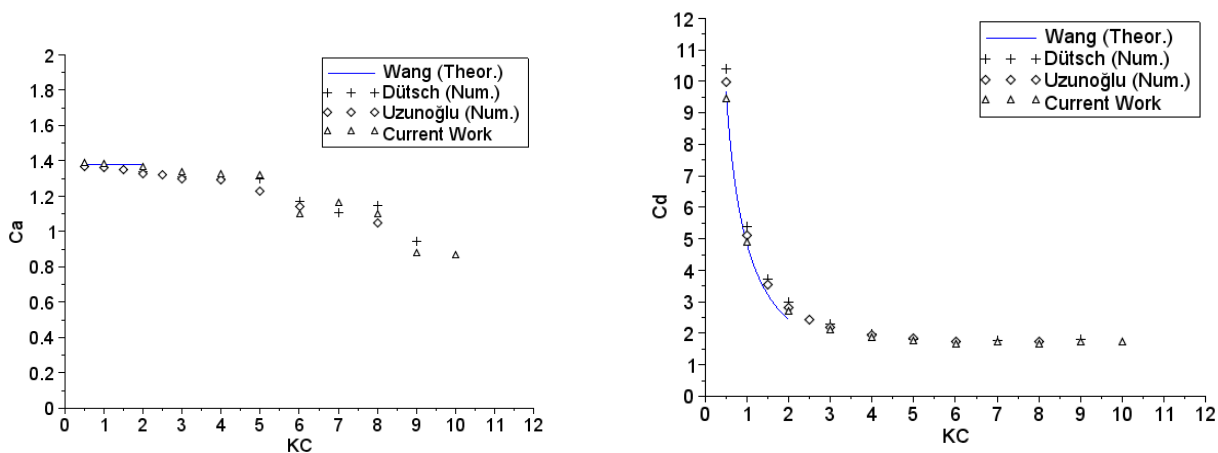


Figure 5. Added mass (left) and drag (right) coefficients

Figure 6 shows the vorticity field for  $0.5 \leq KC \leq 10$ . The evolution of the flow structures with  $KC$  can be clearly observed. Asymmetric flow develops for  $KC \geq 6$ . Due to the limited number of cycles simulated, the regime C was not fully developed, neither a switching to the transverse and diagonal vortex pattern was observed. For low  $KC \leq 2$ , the flow is symmetric and stable. For intermediate  $KC$ , in the range 3 to 5, the boundary layer detaches from the cylinder surface and vortices are shed each half cycle. For higher  $KC$ , between 6 and 10, certain asymmetry develops and vortices are shed obliquely, each half cycle.

For the asymmetric regimes,  $KC \geq 6$ , phase diagrams of in-line versus normal components of the resultant force are shown in figure 7. The normal component has the same order of magnitude as the in-line component. Furthermore, higher harmonics are present in the normal component. If the cylinder were elastically mounted in the transverse

direction, the normal force would give rise to vibrations in this direction (Sumer and Fredsoe, 1988). Such phenomenon may play an important role in the dynamics of risers, in offshore engineering; see, e.g., (Fernandes et al, 2010) or (Rateiro et al, 2013).

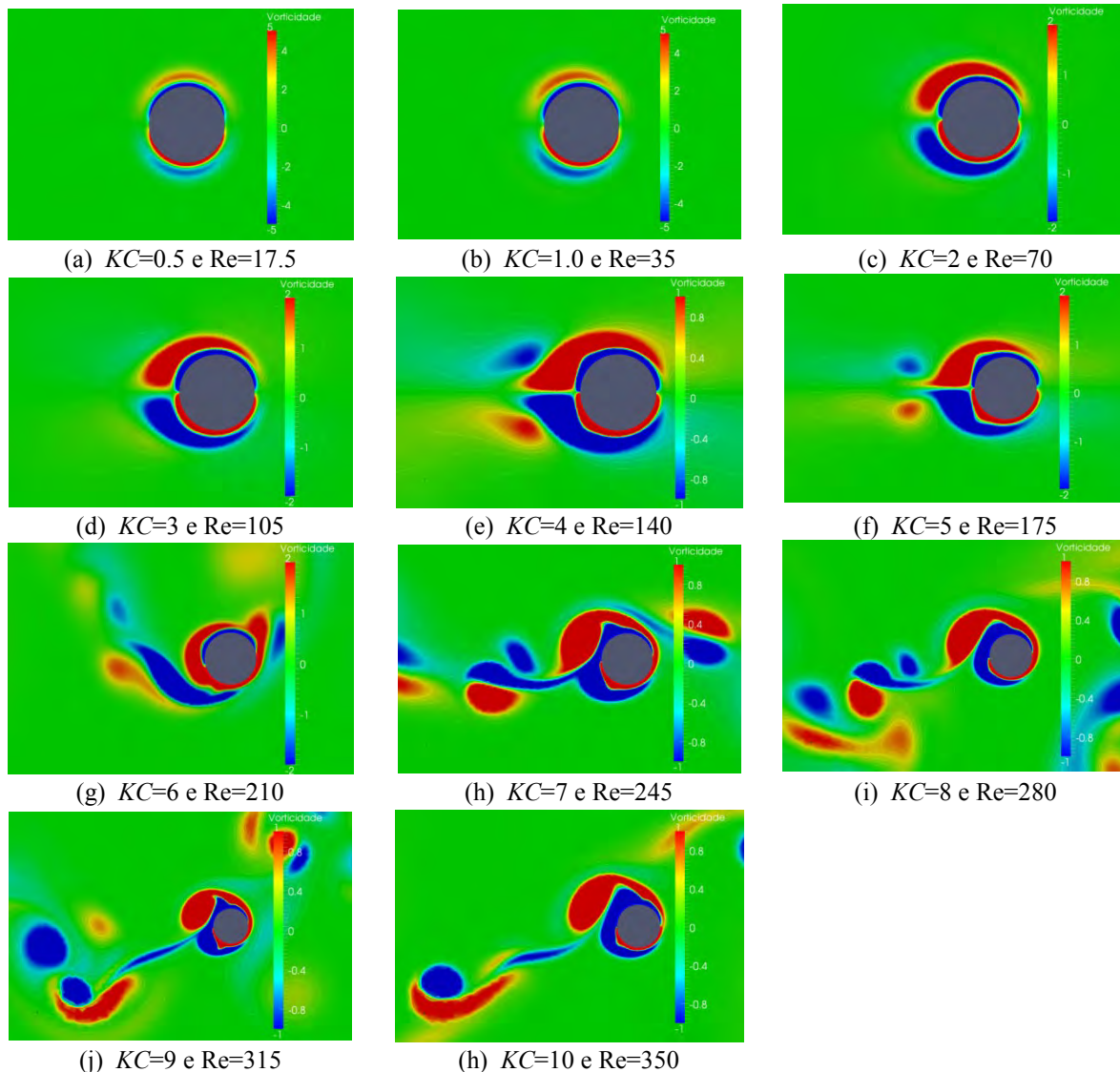


Figure 6. Typical vorticity fields for different flow regimes, respectively: A\*, A\*, A\*, A, A, C, D, F, F, F, F

## 5. CONCLUSIONS

Viscosity indeed affects added mass. In a first moment, through an apparent increase of the cylinder diameter caused by the boundary layer. Later, with increasing amplitude of movement of the cylinder, viscosity affects added mass through the development, growing and shedding of vortices. These vortices changes significantly the flow field near the cylinder and the resulting reactive fluid force.

Numerical simulations were performed for the flow around a circular cylinder forced to move in harmonic oscillation in the range  $17.5 \leq Re \leq 350$  and  $0.5 \leq KC \leq 10$  with a constant frequency parameter  $\beta=35$ . The complexity of the flow increases with  $KC$ . The numerical method showed to be robust and precise. The results agree well with former analytical, experimental and numerical works available in the literature. Although two dimensional, the simulations captured some important vortical flow features in the regimes A\*, A, D and F of Tatsuno and Bearman, recovering quite well added mass and drag coefficients of the Morison's equation.

The normal components of the resultant force appeared for  $KC \geq 6$  in the asymmetric regimes, D and F. It has the same order of magnitude as the in-line component and a more complex energy spectrum, with higher harmonics. In case



the cylinder had a degree of freedom in the normal direction, the normal force could excite the movement and lead to what is sometimes called a vortex self induced vibration of the cylinder.

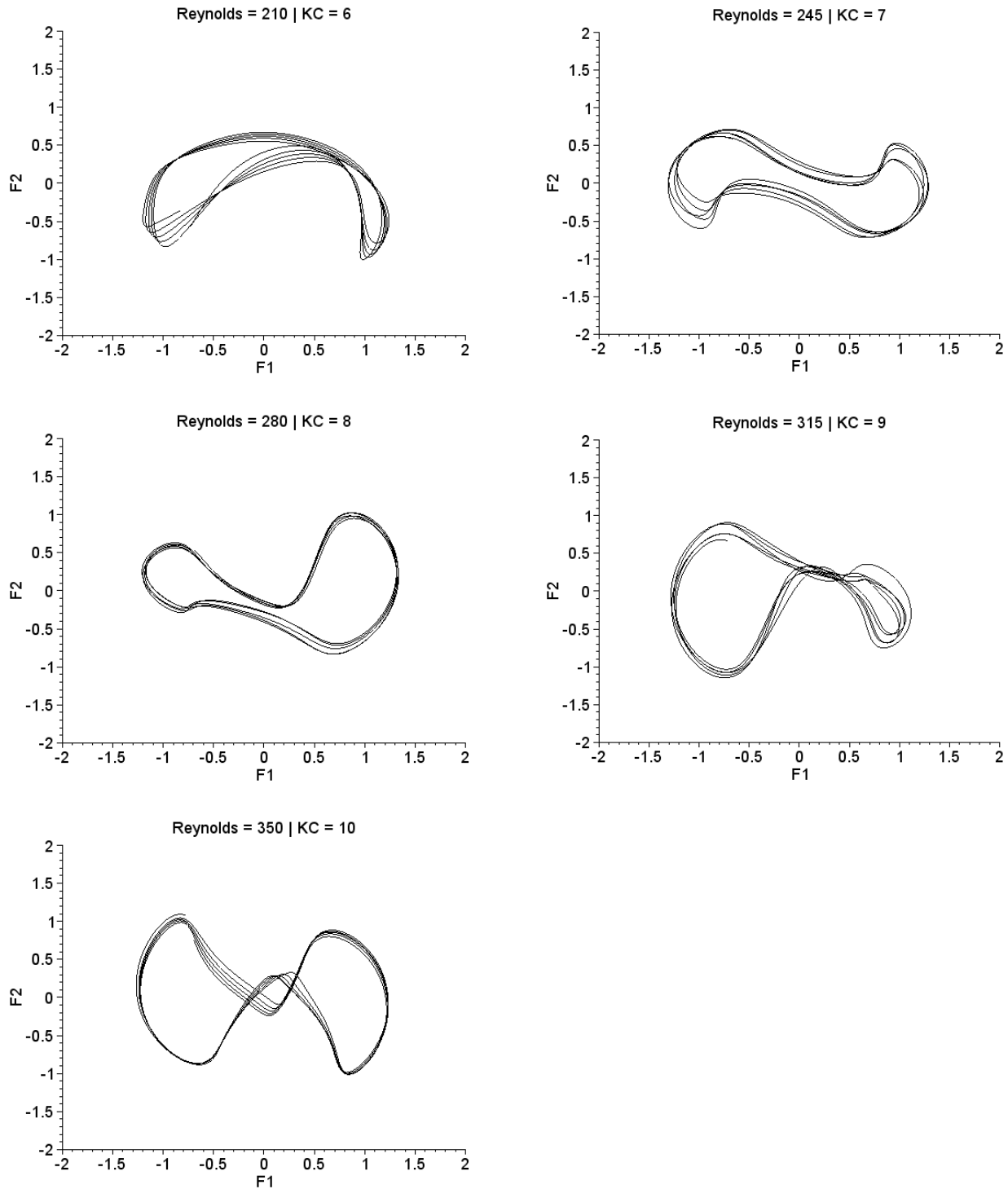


Figure 7. Phase diagrams for the in-line and normal components of the resultant force.  
( $F_1$  and  $F_2$  were made non-dimensional by dividing them by  $\rho DU^2$ )



## ACKNOWLEDGMENTS

The first author acknowledges Voith Hydro for encouraging the research in such a fundamental and classic topic, towards a MSc degree. The second author acknowledges CNPq, research grant number 30.3838/2008-6.

## 6. REFERENCES

- Dütsch, H.; Durst, F.; Becker, S.; Lienhart, H. (1998) "Low-Reynolds-number flow around an oscillating circular cylinder at low Keulegan-Carpenter numbers" *Journal of Fluid Mechanics* Vol. 360.
- Fernandes, A. C., Sefat, S. M., Cascão, L. V., Boas, P. V., & Franciss, R. (2011), "Further investigations on Vortex Self Induced Vibration (VSIV)", *Proceedings of the 30th International Conference on Ocean, Offshore and Arctic Engineering*. Rotterdam, The Netherlands, OMAE2011-50187.
- Ferziger, J.H. (1998) *Numerical methods for engineering application*, Wiley Interscience, 2<sup>o</sup> ed.
- Green, G. (1833) "Researches on the vibration of pendulums in fluid media" *Trans. Royal Soc. Of Edinburgh*.
- Gresho, P.M., Sani, R.L. (2000) *Incompressible flow and the finite element method*, John Wiley, Vol. I and II.
- Korotkin, A.I. (2010) *Added masses of ship strictures*, Springer.
- Lamb, H. (1932) *Hydrodynamics*, Dover Publications.
- Li, L., Sherwin, S.J., Bearman, P.W. (2000) "A moving frame of reference algorithm for fluid/structure interaction of rotating and translating bodies" *Int. Journal for Numerical Methods in Fluids* Vol. 38.
- Lighthill, M.J. (1986) "Fundamentals concerning wave loading on offshore structures" *Journal of Fluid Mechanics* Vol. 173.
- Lin, X.W., Bearman, P.W., Graham, J.M.R. (1996) "A numerical study of oscillatory flow about a circular cylinder for low values of beta parameter" *Journal of Fluids and Structures* Vol. 10.
- Morison, J.R., Johnson, J.W., Schaaf, S.A. "The force exerted by surface waves on piles" *Petroleum Transactions* Vol. 189.
- Rateiro, F., Gonçalves, R.T., Pesce, C.P., Fajarra, A.L.C., Franzini, G.R., Mendes, P. (2013), "A model scale experimental investigation on Vortex Self Induced Vibrations (VSIS) of catenary risers", *Proceedings of the 32<sup>nd</sup> International Conference on Ocean, Offshore and Arctic Engineering*. Nantes, France, OMAE2013-10447.
- Sarpkaya, T. (1976) *In-line and transverse forces on smooth and sand-roughened cylinders in oscillatory flow at high Reynolds numbers*, Naval Postgraduate School, Monterey, California.
- Sarpkaya, T. (1977) "In-line and transverse forces on cylinders in oscillatory flow at high Reynolds numbers" *Journal of Ship Research* Vol. 21.
- Sarpkaya, T. (1986) "Force on a circular cylinder in viscous oscillatory flow at low Keulegan-Carpenter numbers" *Journal of Fluid Mechanics* Vol. 165.
- Sarpkaya, T. (2010) *Wave forces on offshore structures*, Cambridge.
- Stokes, G.G. (1850) "On the effect of internal friction on the motion of pendulums" *Trans. Cambr. Phil. Soc.* Vol. 9.
- Sumer, B. M., & Fredsoe, J. (1988), "Transverse vibration of an elastically mounted cylinder exposed to an oscillating flow" *Journal of Offshore Mechanics and Arctic Engineering*, Vol. 110, pp. 387-394.
- Tatsuno, M., Bearman, P. (1990) "A visual study of the flow around an oscillating circular cylinder at low Keulegan-Carpenter numbers and low Stokes numbers" *Journal of Fluid Mechanics* Vol. 211.
- Uzunoglu, B., Tan, M.; Price, W.G. (2001) "Low-Reynolds-number flow around an oscillating circular cylinder using a cell viscous boundary element method" *Int. Journal for Numerical Methods in Engineering* Vol. 50.
- Wang, C.-Y. (1968) " On high frequency oscillating viscous flows " *Journal of Fluid Mechanics* Vol. 32.

## 7. RESPONSIBILITY NOTICE

The authors are the only responsible for the printed material included in this paper.